INTEGRATING OPTICS AND BIOLOGY: ESTIMATION OF BIOLUMINESCENCE LEAVING RADIANCE FROM AN AUTONOMOUS VERTICAL PROFILER

M. A. Moline[1], T. Bergmann[2], W. P. Bissett[3], J. Case[4], C. Herren[4], C. D. Mobley[5], M. Oliver[2], O. M. E. Schofield[2] and L. Sundman[5]

[1]Biological Sciences Department, California Polytechnic State University, San Luis Obispo, CA 93407
[2]Coastal Ocean Observation Laboratory, Institute of Marine and Coastal Sciences Rutgers University, New Brunswick, NJ 08901
[3]Florida Environmental Research Institute, 4807 Bayshore Blvd. Suite 101, Tampa, FL 33611
[4]Marine Science Institute, University of California, Santa Barbara, CA 93106
[5]Sequoia Scientific Inc., Westpark Technical Center, 15317 NE 90th Street, Redmond, WA 98052

ABSTRACT

Bioluminescence leaving radiance is a function of the temporal and depth-dependent variability of both the in situ bioluminescence potential and the absorptive/scattering properties of the water. During the summers of 2000 and 2001 a suite of sensors were deployed on an autonomous robotic node system located 5km offshore of the New Jersey coast. Data from a newly designed bathyphotometer, an AC-9 and a Hydroscat were taken every 20-30 minutes over the summer experiments to examine the interaction between the bioluminescent signal and the inherent optical properties (IOPs). A modified implicit inverse one-dimensional radiative transfer model combines, meteorological conditions and the bioluminescence potential signal with the IOPs to solve for the first time spectral bioluminescence leaving radiance simultaneously from all depths of the water column on these fine temporal scales. Variation in the vertical structure of bioluminescence potential resulted from a combination of the circadian rhythm of bioluminescence, diel vertical migration, and vertical density structure, with longer temporal variation coherent with episodic (week-scale) physical forcing events. Inherent optical properties also varied in response to these episodic events, with tidal forcing, terrestrial runoff and phytoplankton biomass accumulation influencing both absorption and scattering on shorter time scales (daily). Bioluminescence leaving radiance from each depth reflected these changes over both seasons. The relative effect of the biology and optical properties will be addressed as well as the spectral propagation of light from depth.

INTRODUCTION

Bioluminescence in the ocean is the result of biologically-generated photons from a chemiluminescent reaction. It is produced by over 700 genera representing 16 phyla, spanning the range of small single cell bacteria to large vertebrates (Herring 1987). The reasons for these luminous displays appear to be as varied as the organisms themselves, and may be divided into basic categories of predator avoidance, prey attraction, and

intraspecies communication (Burkenroad 1943, Morin 1983, Abrahams and Townsend 1993). A ubiquitous feature of most of these organisms is that mechanical stimulation will cause organisms to generate light. As many of these organisms are widely distributed in high concentrations, brilliant displays of light as seen in the wakes of ships, in breaking waves, or even around the bodies of rapidly moving dolphins (Rohr et al. 1998). The bioluminescence water-leaving radiance (BLR) for light generated below the surface at any given location is a function of the temporal and depth-dependent variability of both the *in situ* bioluminescence potential and the absorptive/scattering properties of the water.

There have been significant advances in the development of optical sensors, fueled, in part, by the need for in-water validation of ocean color satellites, as well as the Naval need to define the inherent optical properties (IOPs) for visibility and performance prediction modeling (Maffione, 2001; Dickey and Chang, 2001). The most significant advances in optical instrumentation have been the development of sensors that can directly measure *in situ* IOPs. The suite of readily available instrumentation, such as the AC-9, HydroScat, and ECO-VSF, can now directly measure spectral absorption, attenuation, scattering, and backscattering. Independent from the advances in optical instrumentation, relatively compact bioluminescence bathyphotometers have been developed to quantify stimulated light from a fixed water volume. To quantify the potential variability of BLR, simultaneous measurements of both *in situ* IOPs and bioluminescence potential must be made. In addition to sensor development, there has been a concerted effort to develop user-friendly radiative transfer modeling programs for use by the general science community. An example of these programs, Hydrolight (Mobley 1994), was modified for this study to distribute internally generated plane parallel photons (measured bioluminescence) to yield an estimate of BLR (Stephany et al. 2000). This modified implicit inverse one-dimensional radiative transfer model combines measured meteorological data, the bioluminescence potential and the IOPs to solve, for the first time, spectral BLR simultaneously from all depths. This effort was conducted in 2000 and 2001 as part of the Hyperspectral Coupled Ocean Dynamics Experiments (HyCODE) program, designed to utilize hyperspectral imagery to improve understanding of the diverse processes controlling IOPs and the influence of changing IOPs in the coastal ocean.

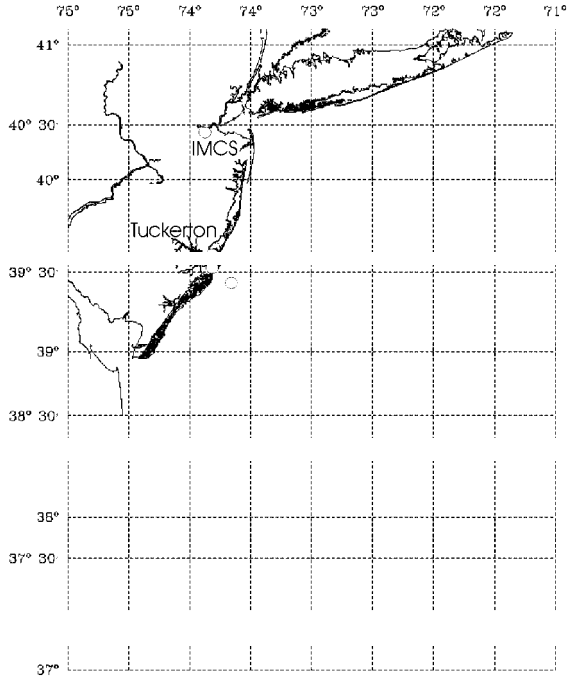

Figure 1. The Long-term Ecosystem Observatory (LEO-15) study site.

METHODS

A robotic vertical profiler was one of the platforms integrated into the

coastal observatory at the Long-Term Ecosystem Observatory (LEO-15) site during the 2000 and 2001 summer field experiments (Figure 1). The profiler was deployed 10km offshore in 13m of water at 39°27.41 N, 74°14.75 W. The profiler frame was anchored to the seafloor with instrument packages attached to a floating drogue which was depth controlled by an attached winch (Figure 2). One of two existing nodes provided the power and data transfer capabilities to the profiler via an electro fiber-optic cable connected to shore. Relevant to this study, the profiler instrument package consisted of a Wetlabs nine wavelength absorption/attenuation meter (ac-9; 412, 440, 488, 510, 532, 555, 650, 676 and 715 nm), a Wetlabs volume scattering meter ECO-VSF, a backscatter/fluorometer HOBI Labs HydroScat-2 (470 nm and 676 nm), and a bioluminescence bathyphotometer. The bathyphotometer pulls water through a 0.5L detection chamber, with a residence time of 1 sec, and a photomultiplier tube incorporated into the chamber measures the total simulated light within the chamber. The ac-9 and HydroScat were factory calibrated and the ac-9 was clean water calibrated prior to the experiment each year. Absorption data were integrated with concurrently collected temperature data and were temperature (Pegau et al. 1997) and scattering [subtraction of a715 from all a channels (Zaneveld and Kitchen 1994)] corrected and binned to 0.25m depth intervals.. Because of the abundance of gelatinous zooplankton in the water column, ac-9 data was filtered to remove spurious spikes in the data. This removal of data from this filtering was rare and represents less than 2% of the total data set. Bioluminescence data (along with optical measurements) were only collected during nighttime profiles (2100-0500) local time. In 2000, the profiler was deployed for ~15 days logging 339 nighttime profiles while in 2001, it was deployed for ~8 days logging 132 nighttime profiles.

Figure 2. Profiler used in study. Instrument cage is on left and winch on the right of the profiler.

To quantify the impact of IOPs and bioluminescence on spectral BLR (380-700 nm), a new bioluminescence module was integrated into the HydroLight v. 4.2 radiative transfer model. The model settings used 0.25 m binned absorption, attenuation, backscatter, volume scattering and bioluminescence data, as well as measured 10m elevation wind velocities from the Rutgers University Marine Field Station to estimate sea surface roughness. Model runs used Pope and Fry (1997) pure water absorption values. The Hydrolight model computed a new spectral scattering phase function when the backscatter to total scatter ratio changed by more than 0.005. Default atmospheric parameters were used for all runs. The current version of Hydrolight has a user option to include bioluminescence in the model run, however, the bioluminescence profile is

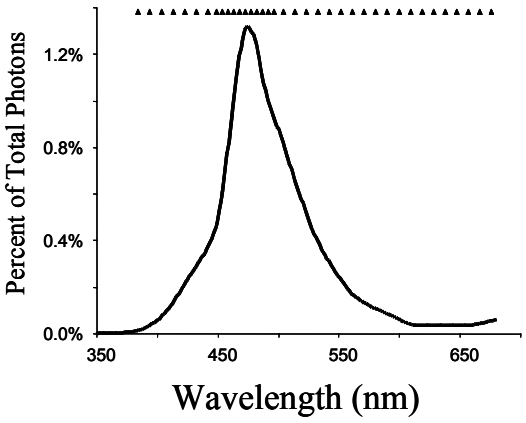

Figure 3. Bioluminescence spectra used as input to Hydrolight. The diamonds above indicate the modeled wavelengths. Data for this spectra were from bioluminescent phytoplankton and copepods isolated and measured in a spectral luminescence sphere.

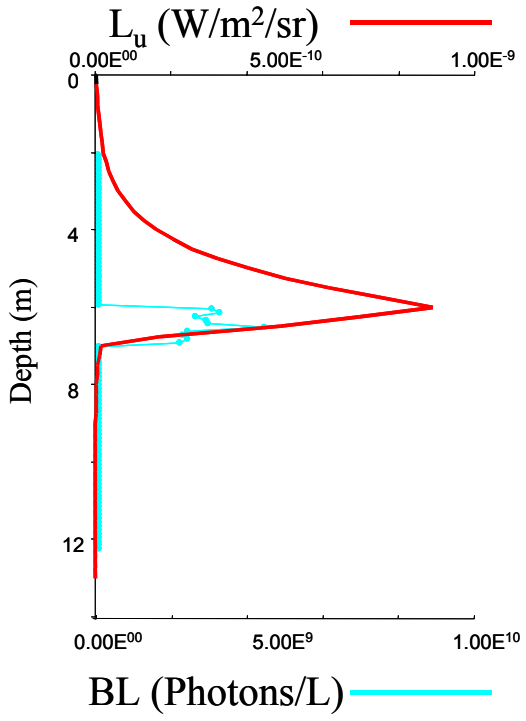

Figure 4. Example of Hydrolight leaving radiance (Lu) output. Measured bioluminescence (BL) measured 1 m above 7m is propagated to the surface.

created from idealized Gaussian functions and the computed solution of leaving radiance is based on "stimulation" of the entire water column bioluminescence. For this study a module was written to allow bioluminescence data to be a user input parameter, as are the IOP inputs, and to distribute these plane parallel photons for propagation in the water column. The model was layered into 1 m sections to simulate more realistic stimulation of the bioluminescent organisms, where specific locations in the water column (1 m thick in this case) were stimulated, rather than the entire water column. This layering decomposed each bioluminescence profile into thirteen 1 m sections and allowed for the calculation of surface BLR of the entire water column if only discrete portions of the water column were emitting bioluminescent light. An example of this data processing is as follows.

Profiles of bioluminescence were spectrally reconstructed using known spectra from a range of dinoflagellate and copepod bioluminescence emission spectra (Figure 3). For this study the spectral shape of the bioluminescence emission spectrum consisted of 36 wavelengths from 380 nm to 680nm. For each meter of every profile the bioluminescence was then propagated upward through the surface waters for the 36 wavelengths using measured values of spectral absorption, attenuation, scattering, backscattering and sea state conditions as inputs into Hydrolight (Figure 4). As the BLR was calculated for each meter, requiring a different set of input files, a single Hydrolight run was needed for each condition. For this study, 7,491

Hydrolight runs were conducted to estimate the spectral BLR for the 2000 and 2001 experiments.

RESULTS AND DISCUSSION

Variation in the vertical structure of bioluminescence potential over each of the two summer experiments resulted from a combination of the daily circadian rhythm of bioluminescence, diel vertical migration of bioluminescent organisms, and vertical density structure, with longer-term changes (week-scale) coincident with episodic upwelling/downwelling.

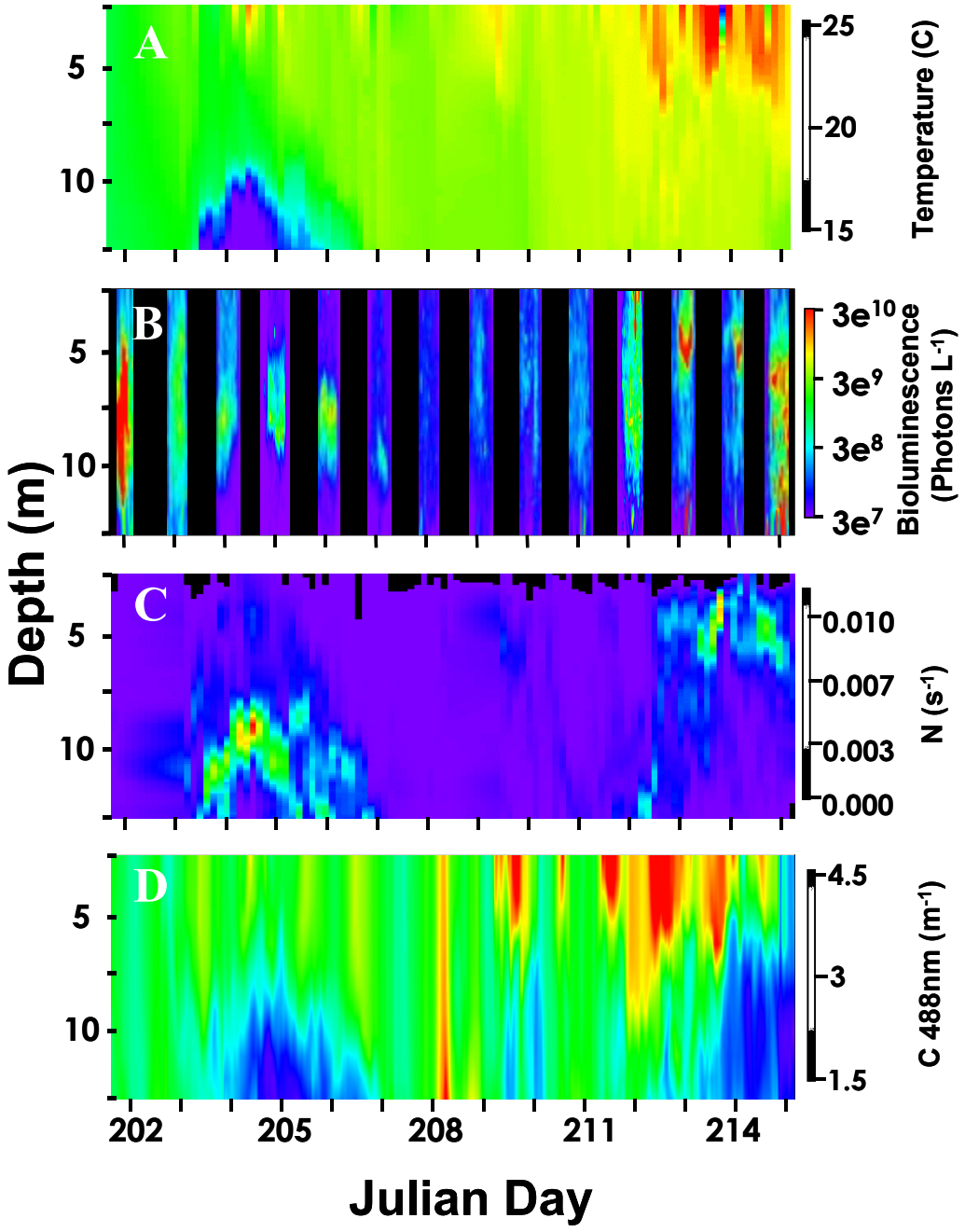

Figure 5. Time series of vertical profiles during 2000 A) Temperature, B)Bioluminescence, C) Buoyancy Frequency and D) Attenuation @ 488nm. JD 001 = Jan 01

Summer 2000

Bioluminescence potential, as well as thermal fine structure, both showed a full range of vertical distribution from stratified layers to homogeneous distributions over the course of the two-week deployment. The water column was well mixed when the instrument was deployed and remained so until the Julian Day (JD) 204, when an intrusion of deep water from the shelf pushed up along the coast in response to upwelling winds from the southwest (Figure 5A). This cold-water intrusion dissipated after three days and was replaced by a warm well mixed homogenous water column. From JD 207 until 212, the water column remained mixed and warmed ~1.5 °C. Over the course of the deployment, surface temperatures warmed from 18 to 24 °C. On JD 202, relatively low BL signals were associated with the mixed water column and the distribution of bioluminescent organisms extended from the surface to 14 m (Figure 5B). As the cold water intrusion from the shelf intensified, the bioluminescent communities were layered and through JD 207 were strongly associated with the maximum density gradients

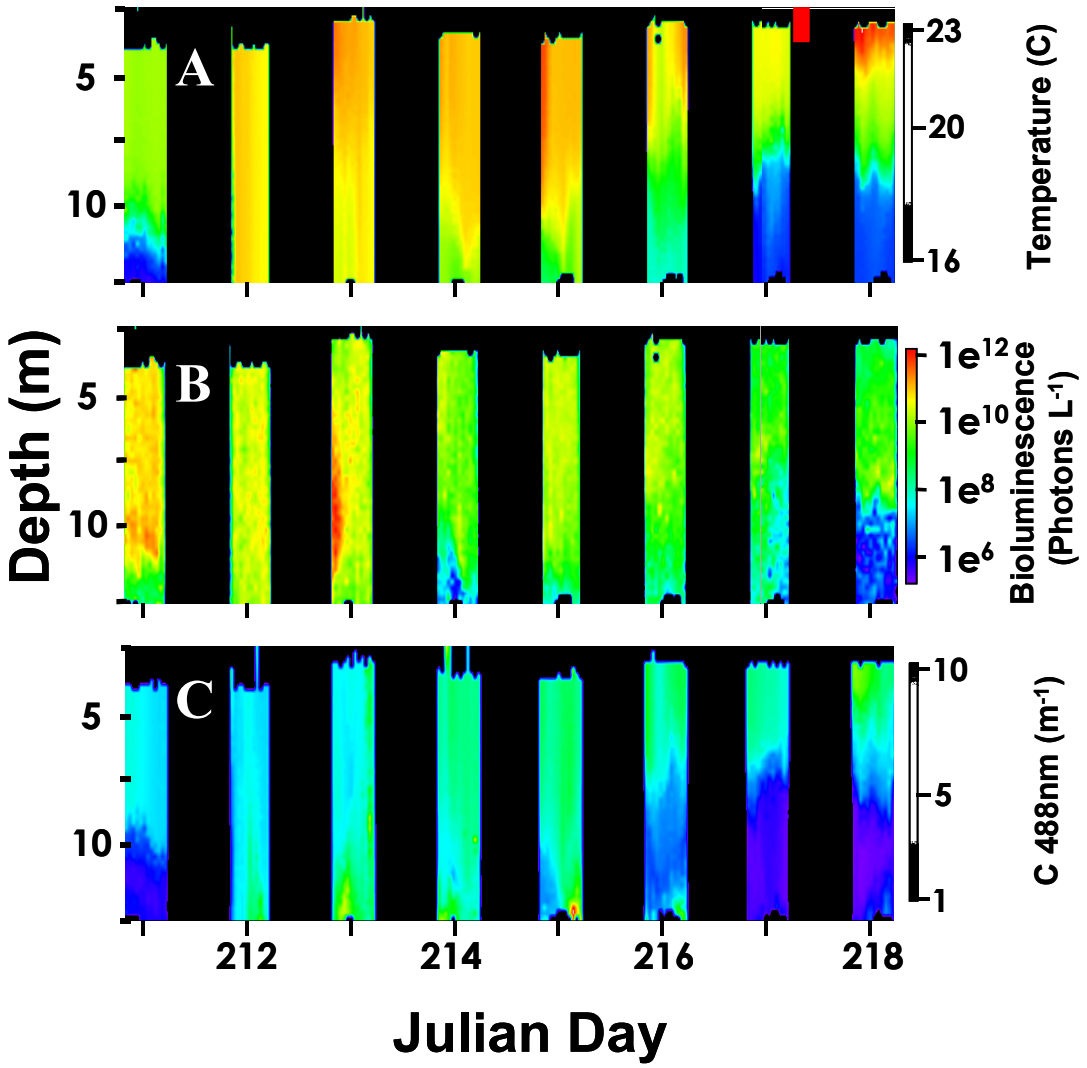

Figure 6. Time series of vertical profiles take during 2001 of A) Temperature, B)Bioluminescence and C) Attenuation at 488nm.

(Figure5C). With the disappearance of the cold bottom water, there was a 3-4 order of magnitude decrease in BL signal. Warming of the surface layer and stratification during the final 4 days of the experiment was related to the development of another layer of high BL potential associated with the thermocline. This warm surface layer was a plume of fresh water discharge from the Hudson River to the north (Oliver et al., submitted).

Despite the different mechanisms for the two periods of stratification during the 2000 experiment, the bioluminescence potential responded similarly. There was a homogeneous distribution of bioluminescence on the final day of the study that coincided with a decrease in stratification resulting from increased wind stress (data not shown). IOPs also varied in response to these episodic events. High attenuation throughout the water column was generally associated with downwelling events with the lowest attenuation in the upwelling bottom water intrusions (Figure 5D). The highest attenuation (>4 m^{-1}) was seen during JD 212-214 when the Hudson River plume extended southward along the coast into our study site.

Summer 2001

The period sampled in 2001 was dominated by downwelling conditions, with warm water extending throughout the water column (Figure 6A). A stratification of the water column was evident the first day of sampling as well as JD 217 and 218. Bioluminescence was on average an order of magnitude higher than the previous year with maximal bioluminescence potential occurring once again at the maximum physical gradients (Figure 6B). As with the temperature, bioluminescence was relatively uniform throughout the water column during downwelling conditions. Attenuation was higher than the previous year and showed a pattern consistent with both the temperature and bioluminescence with higher values generally associated with surface waters (Figure 6C). The highest attenuation was associated with bottom resuspension due to tidal forcing.

BLR from each depth reflected the relative changes in biology and optical properties throughout the water column over both seasons (Figure 7A&B). During 2000, BLR was high due to high bioluminescence and relatively uniform IOP distributions. As the bioluminescence stratified, the maximal leaving radiance was along the density gradients in response to the cold-water intrusion. In mixed conditions, the leaving radiance was proportional to depth as both the light and the IOPs were similar throughout the water column. BLR increased in the last three days of the deployment due to increasing bioluminescence along the pycnocline. Although total attenuation remained high during the day, attenuation measured at night decreased, allowing photons generated deeper in the water column to propagate to the surface. Despite higher bioluminescence in 2001, BLR was approximately half that of 2000 as a result of high attenuation. Attenuation generally increased while bioluminescence decreased, leading to a trended decrease in the BLR over time (Figure7B). The highest leaving radiance from depth was on JD 213.

As with the spectral shift in solar radiation with depth, results here quantify that there is a significant shift of over 80nm from blue to green as light propagates to the surface. Maximal bioluminescence occurs at ~474 nm, however as the depth of the bioluminescence source increases and that the proportional BLR at 474nm relative to 555nm is 40-fold less for sources at depth. Figure 7C illustrates this spectral shift with

depth and the variation that occurs in response to environmental dynamics. The most striking spectral differences occur when the water column is optically stratified, with higher attenuating surface water and clearer bottom water. During these conditions, for

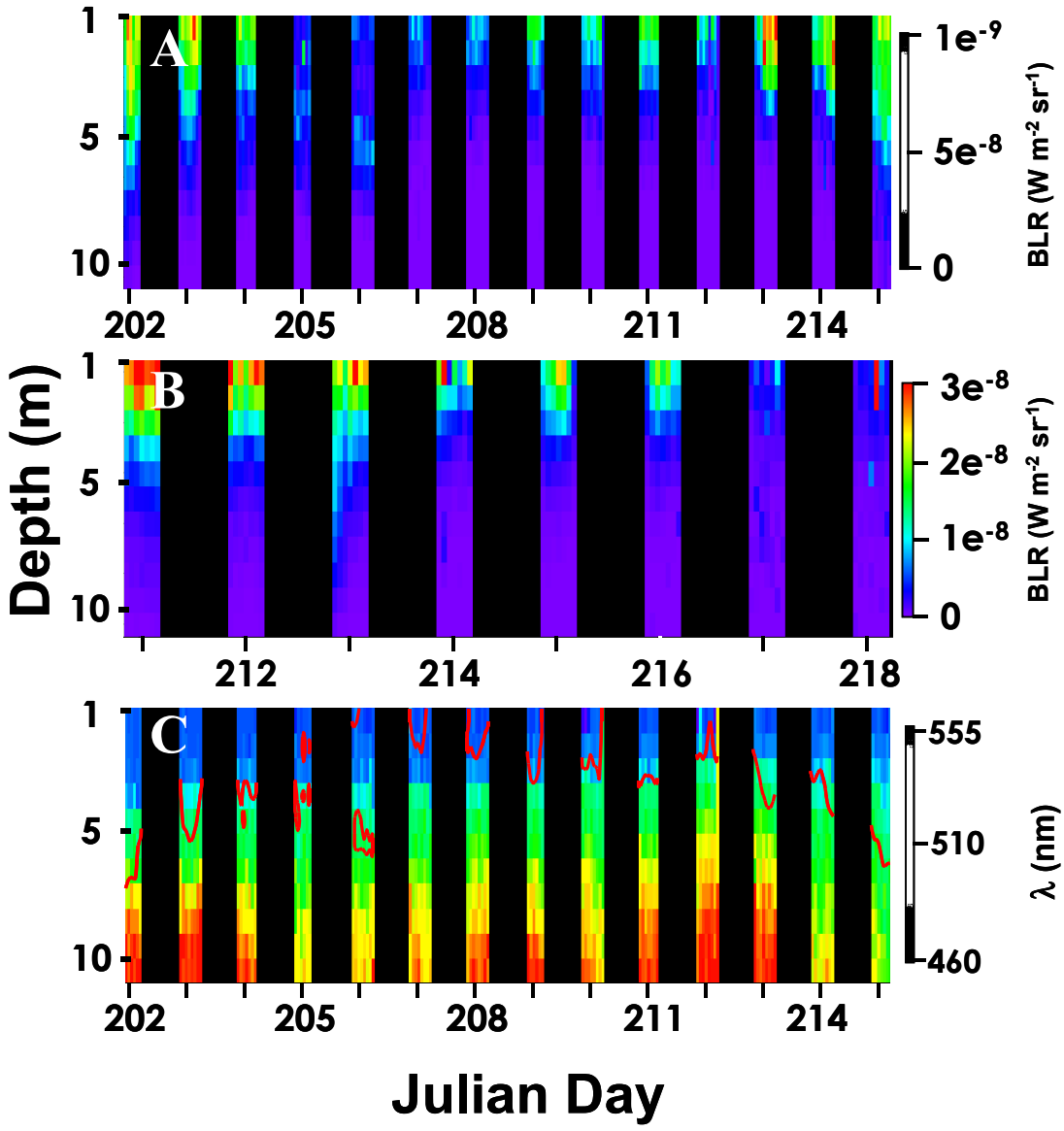

Figure 7. Time series of vertical profiles of bioluminescence water leaving radiance (BLR) take during the summers of A) 2000 and B) 2001. C) Time series of the depth distribution of the maximum wavelength of the BLR. Overlaid (red lines) are the depth contours of BLR of 1 e^{-8} ($W\ m^{-2}sr^{-1}$).

example JD 205 & 214, blue BLR occurs at nearly all depths. During downwelling conditions, maximum BLR wavelengths (greater than 540nm) are from as shallow as 5 meters (JD 212). This has significant implications for the development of sensors designed to quantify BLR, as some sources at depth will have a significantly different spectral signatures. These findings from a single optically deep study area, suggests that

the development of shore-based, ship-based, and/or airborne bioluminescence sensors (LLLII; Lynch 1981) should include the spectral range required to quantify surface stimulated bioluminescence as well as bioluminescence stimulated at depth. The actual spectral range will ultimately depend on the sensitivity of the instrument.

CONCLUSIONS

Results provide a qualitative picture of the significant variability in the BLR over time and emphasize the need for more simultaneous measurements of bioluminescence potential and IOPs in coastal regions. Additional studies are needed to quantify the proportional contributions that IOPs and bioluminescence potential make to BLR under varying environmental conditions.

Hydrolight, as employed here, assumes a continuous uniform layer of bioluminescence in the calculations. While results here are a good first step in examining qualitative changes in BLR and show clear spectral shifts, a more rigorous approach is needed for a quantitative solution. In particular, if bioluminescence is consider a point source function rather than a plane source function, then a Monte Carlo-type approximation is required to incorporate the vertical and horizontal distribution of light and accurately predict leaving radiance (Gordon 1987). The work of Gordon (1987) was part of the Biowatt/ML-ML program, and illuminates the difficulties inherent in developing radiance models for bioluminescence leaving radiance, as well as possible difficulties in developing the sensors necessary to adequately measure BLR. Given the availability of new *in situ* bioluminescence bathyphotometers and optical sensors, and the increase in computational abilities, an improved theoretical approach should be derived and field validated.

ACKNOWLEDGEMENTS

We wish to thank M. Purcell, C. Von Alt, and C. Johnson for fabrication of the mooring, the Rutgers Marine Field Station and *R/V Arabella* staff for deployment, S. Glenn for the unique ocean observation infrastructure at Rutgers University, and the profiler operators; J. Blackwell, S. Blackwell, A. Briggs, G. Chang, M.Crowley, J. Kohut, K. Oliver, J. Pearson, D. Peterson, E Heine and A. Weidemann. S. Blackwell also assisted with graphics. This study was funded by ONR (N00014-99-1-0197 and N00014-00-1-0008 to M. Moline and N00014-99-1-0196 to O.M.E. Schofield).

REFERENCES

Abrahams, V. A. and Townsend, L. D. 1993. Bioluminescence in dinoflagellates: A Test of the burglar alarm hypothesis. Ecology 74(1):258-260.

Dickey, T. D. and G. C. Chang 2001. Recent advances and future visions: Temporal variability of optical and bio-optical properties of the ocean. Oceanography 14(3): 15-29.

Gordon, H.R. 1987. Bio-optical model describing the distribution of irradiance at the sea surface resulting from a point source embedded in the ocean. App. Opt. 26(19): 4133-4148.

Herring, P. J. 1987. Systematic distribution of bioluminescence in living organisms. J. Biolum. Chemilum. 1: 147-163.

Lynch, R. V. 1981 Patterns of bioluminescence in the oceans. NRL Report 8475, Naval Research Laboratory, Washington D.C., pp. 1-32.

Maffione, R. A. 2001. Evolution and revolution in measuring ocean optical properties. Oceanography 14(3): 9-14.

Mobley, C. D. 1994. Light and Water: Radiative transfer in natural waters. Academic Press, New York, pp. 1-592.

Morin J. G. 1983. Coastal bioluminescence: Patterns and functions. Bulletin of Marine Science 33(4):787-817.

Oliver, M., O. Schofield, T. Bergmann, S. Glenn, C. Orrico and M. A. Moline (submitted) Deriving in situ phytoplankton absorption for bio-optical productivity models in turbid waters. J. Geophys. Res.

Pegau, W., D. Gray and J. Zaneveld (1997). Absorption and attenuation of visible and near-infrared light in water: dependence on temperature and salinity. Applied Optics 36(24): 6035-6046.

Pope, R. and E. Fry. 1997. Absorption spectrum (380-700 nm) of pure water. II. Integrating cavity measurements. App. Opt. 36:8710-8723.

Rohr, J., M. I. Latz, et al. 1998. Experimental approaches towards interpreting dolphin-stimulated bioluminescence. J. Exp. Bio. 201: 1447-1460.

Stephany, S., F. M. Ramos,H. F. C. Velho and C. D. Mobley. 2000. Identification of inherent optical properties and bioluminescence source term in a hydrological optics problem. J. Quant. Spectros. Rad. Trans. 67: 113-123.

Zaneveld, J. and J. Kitchen (1994). The scattering error correction of reflecting tube absorption meters. SPIE 2258: 44-55.